RSC Advances

PAPER

View Article Online
View Journal | View Issue

Cite this: *RSC Adv.*, 2022, **12**, 16153

1-(4-Hydroxyphenyl)-2*H*-tetrazole-5-thione as a leveler for acid copper electroplating of microvia

Xulingjie Teng,[a] Zhihua Tao,*[a] Zhiyuan Long,[a] Guanting Liu[a] and Xuefei Tao[b]

Received 8th April 2022
Accepted 24th May 2022

DOI: 10.1039/d2ra02274e

rsc.li/rsc-advances

Microvia filling by copper electroplating was performed using plating solution with 1-(4-hydroxyphenyl)-2*H*-tetrazole-5-thione (HPTT) as the leveler. Galvanostatic Measurements (GMs), Linear Sweep Voltammetry (LSV) and Electrochemical Impedance Spectroscopy (EIS) tests were carried out to investigate the electrochemical behaviors of HPTT and its synergistic effect with other additives, in comparison with 1-phenyltetrazole-5-thione (PMT). GMs showed a convection-dependent interaction between PEP and HPTT. LSV and EIS tests indicated both HPTT and PMT enhanced the inhibition effect of PEP, and the synergistic effect of HPTT and PEP was stronger than that of PMT. Cross-section images illustrated the filling rate of the microvia with a 150 μm diameter and a 75 μm depth was 95.6% in 60 minutes with HPTT as the leveler. Frontier Molecular Orbitals (FMO) and Electrostatic Potential (ESP) of HPTT and PMT using quantum chemical calculations predicted the reaction sites for electrophilic and nucleophilic attack. Quantum chemical calculations suggested that HPTT is easier than PMT to bond to a copper surface and PEP.

1. Introduction

Copper electrodeposition is of great significance for high-density interconnector printed circuit board (PCB) fabrication.[1,2] The electrical interconnection of conductive layers can be achieved by microvia filling known as superfilling or bottom-up filling. To implement void-free electrodeposition for microvia, introduction of chemical additives such as chloride ion, suppressors (*e.g.* polyethylene glycol (PEG) and triblock copolymer comprised of propylene oxide–ethylene oxide–propylene oxide (PEP)), accelerators (*e.g.* bis-(3-sulfopropyl)disulfide (SPS)) and levelers (*e.g.* Janus Green B, JGB) at low concentration is essential.[3–5]

Chloride ions have an accelerating effect on copper deposition as well as a synergistic effect with the accelerator.[6] At the same time, the suppressor requires the presence of Cl^- to exert its inhibitory effect. Suppressors are generally macromolecular polyether compounds. They are mainly adsorbed on the surface of plated parts, forming an adsorption film with Cl^- that blocks the diffusion of Cu^{2+}.[7] Owing to the competitive adsorption with suppressors, accelerators are mainly adsorbed at the bottom of microvias, reducing the energy for the reduction of copper ions and accelerating copper electrodeposition by the sulfonate group.[8] Indispensable for electroplating systems with suppressors and accelerators, levelers can inhibit copper ion deposition outside the microvia by the synergistic effect with suppressors so as to improve the filling performance.[9] Quaternary ammonium salts are commonly used levelers, including Janus green B (JGB), Diazine black (DB), methylene blue (MB), Alcian blue, (ABPV).[10–12] Commercial application of quaternary ammonium salts as levelers is facing problems of quality and environmental pollution.

Various schemes, for example, low molecular compounds with specific functional groups, have been proposed to address quality and environmental pollution issues.[3,5,13,14] Organic molecules with heteroatoms of nitrogen (N), sulfur (S) and conjugated π–π bonds are adsorbed well on the surface of copper.[15–18] Small molecule levelers with these characteristics, such as 4-amino-2,1,3-benzothiadiazole and 4,6-dimethyl-2-mercaptopyrimidine (DMP), have appeared in previous reports.[19,20] However, they are still in the preliminary research phase and the mechanism of adsorption still remains unclear.

HPTT has a low cost and similar structure to PMT as shown in Fig. 1(a). HPTT is reported as a new leveler herein, with heteroatoms, conjugated π–π bonds, strong molecular polarity. GMs, LSV and EIS tests were carried out to investigate the electrochemical behaviors of HPTT and its synergistic effect with other additives, in comparison with PMT. Microvia filling by copper electroplating were performed using plating solution with PEP, SPS and HPTT as the suppressor, accelerator and leveler respectively. FMO and ESP of HPTT and PMT using quantum chemical calculations predicted the reaction sites for electrophilic and nucleophilic attack.

2. Experimental

2.1. Electrochemical procedures

The electrochemical workstation was CHI608E (Chenhua) and the electrolytic cell was a standard three-electrode cell with

[a]*Department of Applied Chemistry, School of Materials and Energy, University of Electronic Science and Technology of China (UESTC), Chengdu, 610054, China. E-mail: tzh3595@uestc.edu.cn; Fax: +86-28-83201711; Tel: +86-28-83201711*

[b]*Jiangxi Vocational College of Finance and Economics, Jiujiang, 332000, China*

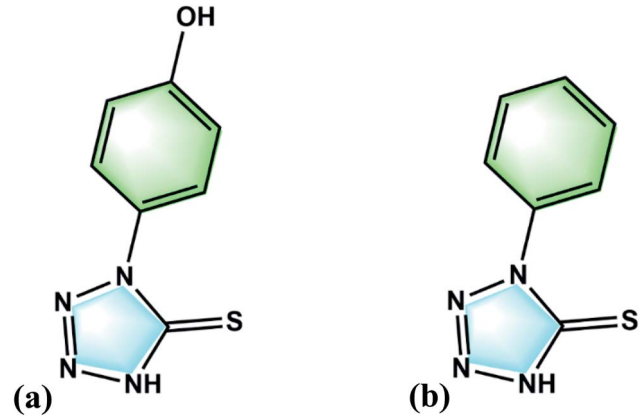

Fig. 1 Chemical structures of (a) HPTT and (b) PMT.

a capacity of 100 mL. Electrochemical experiments contained GMs, LSV and EIS tests. The working electrode (WE) was a platinum rotating disk electrode (Pt-RDE) with an area of 0.196 cm^2. The counter electrode (CE) was a copper rod. A saturated mercuric sulfate electrode (SMSE) served as the reference electrode. The copper rotating disk electrode (Cu-RDE) was prepared by depositing a copper layer of about 500 nm on Pt-RDE before the electrochemical experiments.

GMs were performed on Cu-RDE at 100 rpm and 1000 rpm respectively with a constant current density of 2 A dm^{-2}. The potential difference measured by GMs was defined as eqn (1).

$$\Delta\eta = \eta_{100\text{rpm}} - \eta_{1000\text{rpm}} \quad (1)$$

The working electrode was Cu-RDE when LSV tests were performed. All LSV tests were carried out by reverse scan from −0.35 V to −0.80 V (*vs.* SMSE) at a rate of 1 mV s^{-1}. EIS tests were performed on the Cu-RDE electrode at −0.65 V (*vs.* SMSE) with a frequency range from 0.1 Hz to 100 kHz. The amplitude was set to 5 mV.

2.2. Copper electroplating

The experimental samples were PCBs where the effective size of the microvia was 6 × 8.33 cm^2. The diameters of microvias were 150 μm and 100 μm respectively, and the depth was 75 μm. The anodes were two phosphorus-containing copper boards, placed in a 1.5 L Harring cell where the composition of the virgin make-up solution (VMS) was 0.88 mol L^{-1} $CuSO_4 \cdot 5H_2O$, 0.54 mol L^{-1} H_2SO_4. Prior to metallization, the microvias were cleaned through a decontamination process to remove dirt and oxides, so as to obtain good electrical conductivity at the interface between the filled copper and the inner copper pad. The current density was set to 2.0 A dm^{-2} and the time duration was set to 60 min. Continuous air bubbles at a flow rate of 2.5 L h^{-1} were injected into plating solution during electroplating to ensure sufficient convection intensity. The entire plating process was carried out at 25 °C. Cross-sections of microvias after electroplating were observed by the metallurgical microscopy to evaluate the filling performance of the electroplating solution.

The filling rate (F) of microvias is defined by eqn (2):

$$F = \frac{A}{B} \times 100\% \quad (2)$$

where A is the distance from the top of microvias to the bottom, B is the distance from the bottom of microvias to the surface of PCBs,[21,22] as illustrated in Fig. 2, and C is the electroplating copper thickness on the surface of PCBs.

2.3. Quantum chemical calculations and molecular dynamics simulation

The geometry of HPTT and structures of PEP-HPTT/PMT were optimized with the B3LYP/6-31G (d, p) method in Gaussian 9 software based on density generalized function theory (DFT).[23] The optimized geometry and molecular orbitals were visualized by Multiwfn and VMD software.[24] According to the frontline molecular orbital theory, Lowest Unoccupied Molecular Orbital (LUMO) and Highest Occupied Molecular Orbital (HOMO) were taken into account. The energy difference of the frontline orbits ($\Delta E = E_{\text{LUMO}} - E_{\text{HOMO}}$) was calculated and the ESP mapped surface was plotted.

3. Results and discussion

3.1. Electrochemical evaluation

The potential transients obtained by successive injections of PMT and HPTT into the basic electrolyte are shown in Fig. 3. GMs using a copper working electrode that was individually operated at two different rotation speeds could accurately predict the filling performance of a copper plating formula for microvia filling.[17] The value of $\Delta\eta = \eta_{100\ \text{rpm}} - \eta_{1000\ \text{rpm}}$ can assess the filling performance of the electrolyte on the basis of theoretical analysis of convection-dependent adsorption (CDA). The electrolyte exhibits convection-dependent adsorption when

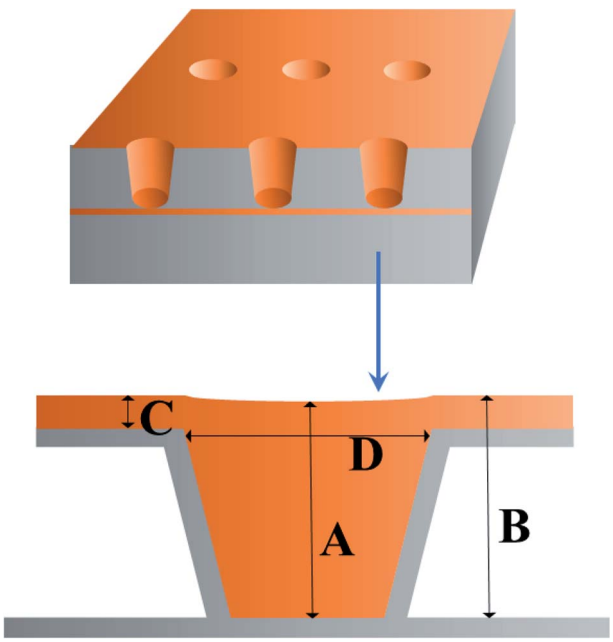

Fig. 2 A general model of microvias.

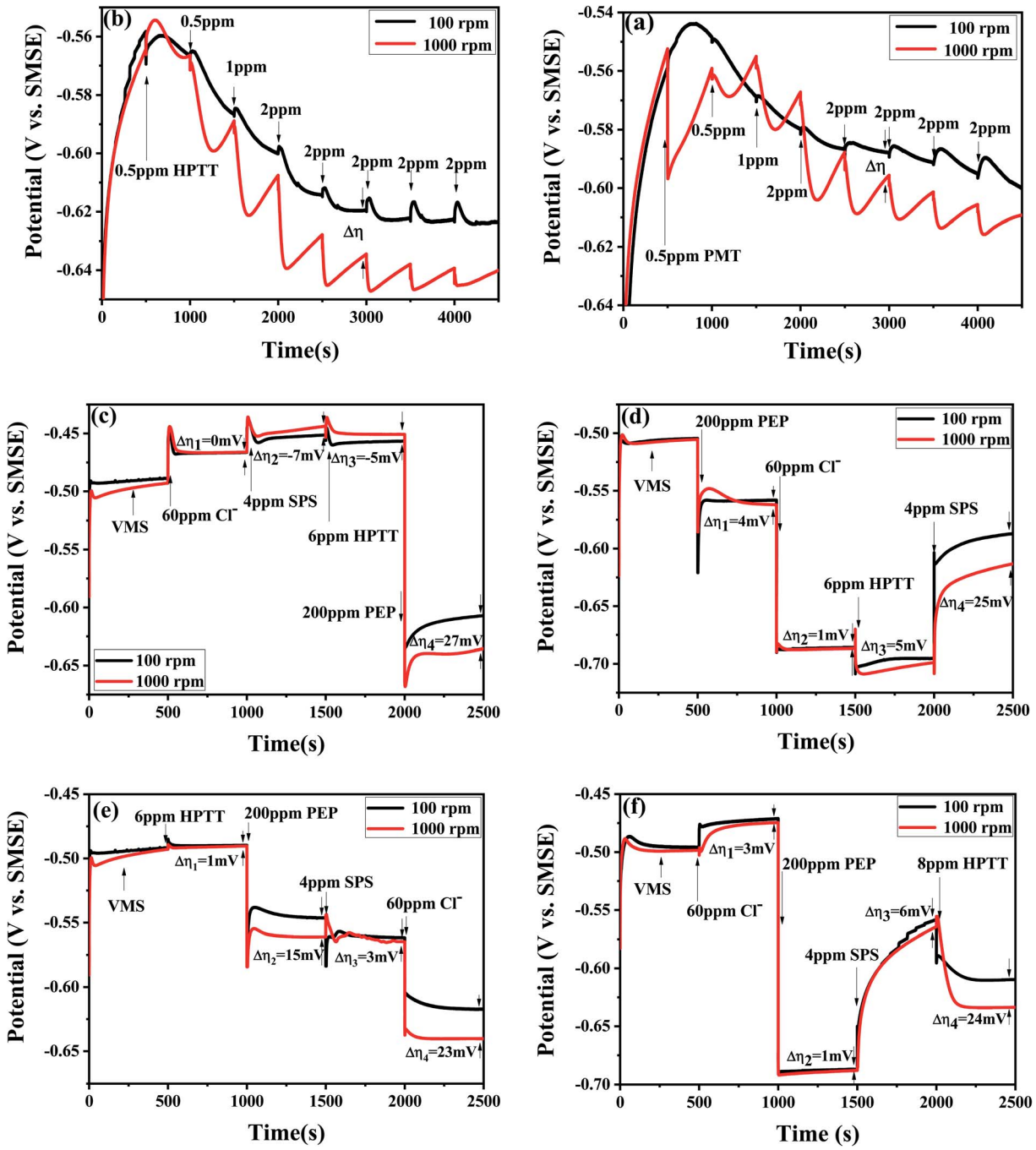

Fig. 3 GMs with the successive addition of various additives at two different rotation speeds: 100 and 1000 rpm.

$\Delta\eta > 0$. In general, the more positive and larger the value of $\Delta\eta$ is, the better the filling performance will be. The electrolyte contains 60 ppm Cl^-, 200 ppm PEP and 4 ppm SPS from 0 to 500 s, as marked in Fig. 3(a and b). There is almost no difference between the deposition potentials at 100 rpm and 1000 rpm, and they both show an increasing trend, suggesting that SPS is slowly replacing the PEP adsorbed on the copper surface. The electrolyte does not show CDA behavior during this process. Fig. 3(a and b) shows a decreasing trend for all four curves when PMT/HPTT are added at 500 s, respectively. The lowest deposition potentials in Fig. 3(a and b) reached about −0.60 V and −0.63 V, respectively, implying that both PMT and HPTT have an inhibitory effect on copper deposition, and the inhibitory effect of HPTT is stronger than that of PMT. In comparison with the two curves in Fig. 3(b), it can be seen that the deposition potential decreases slowly with the addition of HPTT at 100 rpm. It can be explained by the fact that HPTT is slowly replacing the SPS adsorbed on the copper surface throughout

the process, and the adsorption of HPTT is slower than that of SPS at the moment. With the addition of HPTT at 1000 rpm, the curve is wavy and a valley exists every 500 s. This phenomenon can be explained by the fact that the adsorption of HPTT accelerates under strong forced convection and rapidly replaces SPS on the copper surface, followed by SPS gradually replacing HPTT after a period. The above explanation also applies to PMT, therefore, the adsorption rate of both PMT and HPTT on the copper surface is affected by forced convection, and the strong forced convection will accelerate their adsorption rate on the copper surface. This result is favorable for electroplating. At the beginning of plating, the leveler is quickly adsorbed on the copper surface outside microvias where convection is stronger and strongly inhibits copper deposition on the surface, while the leveler at the bottom of microvias is adsorbed more slowly, facilitating the rapid accumulation of SPS at the bottom. More importantly, with the increase of HPTT concentration, $\Delta\eta$ gradually increases and reaches the maximum value at the concentration of 6 ppm, demonstrating that the optimal concentration of HPTT is 6 ppm under the electrolyte system of 60 ppm Cl^-, 200 ppm PEP and 4 ppm SPS. $\Delta\eta$ (HPTT) > $\Delta\eta$ (PMT) indicates that the filling performance of HPTT as a leveler will be better than that of PMT.

The interaction between HPTT and other additives is further investigated in Fig. 3(c–f). The deposition potential increases with injection of 60 ppm Cl^- and 4 ppm SPS into the VMS, as seen in Fig. 3(c), for the reason that Cl^- will be adsorbed on the copper surface rapidly and coordinate with Cu^{2+} and SPS to form SPS–Cu^{2+}–Cl^- complexes, thus transforming the reduction of Cu^{2+} into an inner sphere electron transfer mode.[6,25–29] The subsequent addition of HPTT reveals a 6 mV decrease in the deposition potential, indicating that the addition of HPTT partially attenuates the depolarizing effect of SPS. The negative value of $\Delta\eta_3$ implies that the electrolyte does not have the capability for superfilling. With the addition of 200 ppm PEP at 2000 s, the deposition potential decreases to about 0.63 V and then slowly rises and reaches equilibrium, suggesting that the adsorption of PEP is a rapid process and the competitive adsorption of SPS and PEP is mainly manifested by SPS replacing the adsorbed PEP. The value of $\Delta\eta_4$ equals 22 mV and the electrolyte exhibits CDA behavior. The polarization of PEP on the cathode in the presence of Cl^- is substantially enhanced, as displayed in Fig. 3(d), illustrating the existence of synergistic inhibition between PEP and Cl^-, *i.e.*, the PEP–Cu^+–Cl^- inhibitor is formed.[30] The addition of 6 ppm HPTT at 1500 s reveals a further decrease in the deposition potential, implying a further synergistic inhibition of HPTT and PEP, noted as PEP–HPTT. After injection of SPS at 2000 s, the value of $\Delta\eta_4$ equals 25 mV and the achievement of superfilling is allowed by this electrolyte. These results indicate that HPTT affects the deposition potential in the electrolyte by interacting with PEP, while HPTT itself has no significant effect on the copper deposition.

As shown in Fig. 3(e), HPTT itself has no significant effect on the polarization potential, and $\Delta\eta_2$ equals 14 mV after injection of 200 ppm PEP. Comparing with Fig. 3(d), it can be concluded that there is a convection-dependent interaction between HPTT and PEP, with a superimposed effect on the inhibitory effect of PEP. The value of $\Delta\eta_3$ in Fig. 3(d) is 5 mV since the PEP–HPTT interaction is weaker than PEP–Cu^+–Cl^-, causing its convection-dependent property to be overridden. This PEP–HPTT interaction is eliminated after the addition of 4 ppm SPS at 1000 s, as displayed in Fig. 3(e), indicating that SPS has replaced the adsorbed HPTT or PEP. With injection of 60 ppm Cl^- at 1500 s, the value of $\Delta\eta$ increases substantially and the deposition potential decreases. PEP forms a PEP–Cu^+–Cl^- adsorption layer while binding to HPTT, followed by a competitive adsorption with SPS. The increase in $\Delta\eta$ should be attributed to the predominance of PEP–HPTT adsorption in the strong forced-convection region and the predominance of SPS adsorption in the weak forced-convection region. It can be found that the competitive adsorption of PEP and SPS in the absence of the leveler is not convection-dependent, so the synergistic effect of HPTT and PEP plays a key role in improving the microvia-filling performance, by contrast with the 1500 s to 2000 s phase in Fig. 3(f).

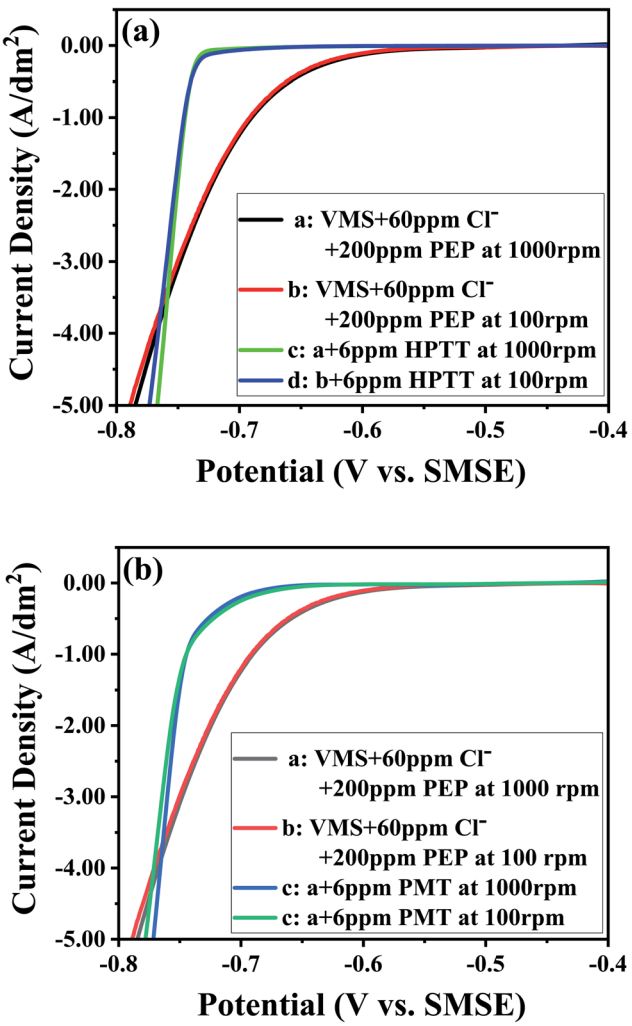

Fig. 4 Linear sweep voltammetry measurements: (a) HPTT and (b) PMT.

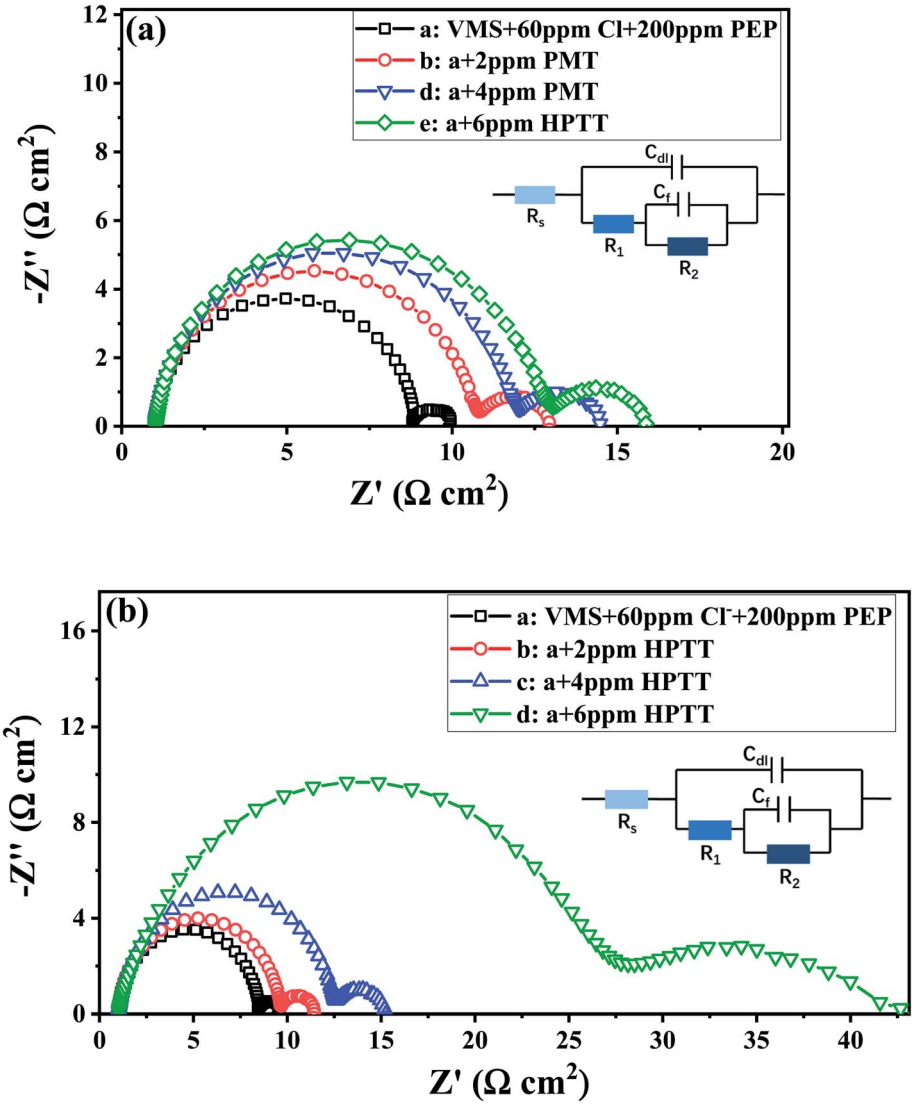

Fig. 5 Nyquist was carried out at −0.65 V with electrolyte composed of 0.88 M $CuSO_4 \cdot 5H_2O$, 0.54 M H_2SO_4, 60 ppm Cl^-, 200 ppm PEP and (a) PMT/(b) HPTT.

Table 1 Electrochemical impedance parameters in plating solution in the presence and absence of PMT and HPTT

C (ppm)	R_s (ohm cm^2)	C_{dl} (10^{-5} F cm^{-2})	R_1 (ohm cm^2)	C_f (F cm^{-2})	R_2 (ohm cm^2)
PMT					
0	0.998	1.84	7.850	0.144	1.064
2	1.001	3.78	9.922	0.039	1.862
4	1.012	2.70	10.994	0.031	2.183
6	1.026	2.67	11.962	0.027	2.568
HPTT					
0	0.985	2.13	7.493	0.124	1.067
2	0.988	2.99	8.695	0.060	1.603
4	0.997	4.47	11.648	0.042	2.350
6	1.014	8.31	27.009	0.013	15.892

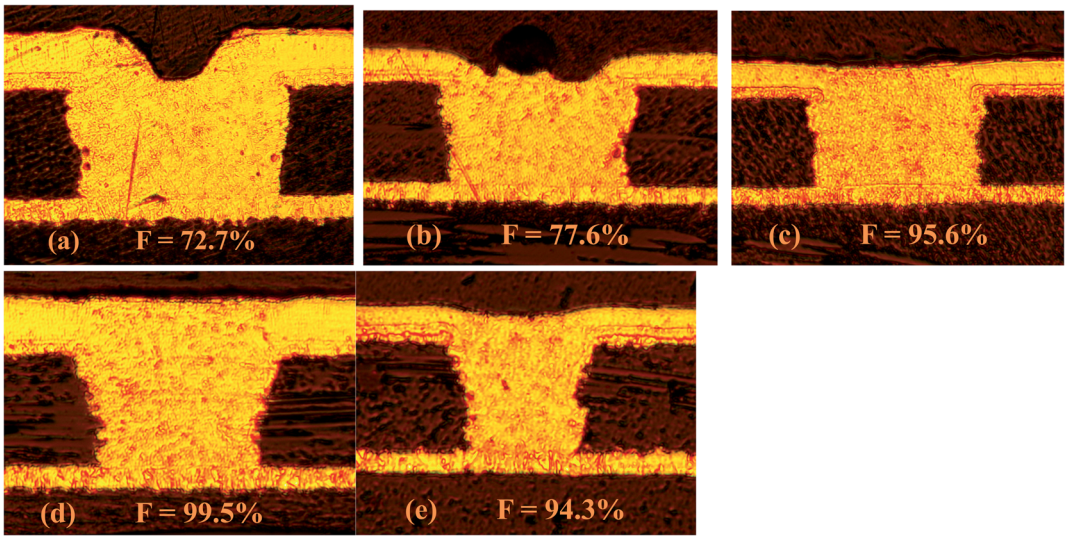

Fig. 6 Cross-section images of microvias with diameters of: (a) 150 μm for 60 min with PMT, (b) 150 μm for 40 min with HPTT, (c) 150 μm for 60 min with HPTT, (d) 150 μm for 80 min with HPTT, (e) 100 μm for 40 min with HPTT. The plating solution is composed of VMS, 60 ppm Cl^-, 200 ppm PEP, 4 ppm SPS and 6 ppm leveler.

To further investigate the synergistic inhibition of levelers with PEP, LSV and EIS tests were performed. The addition of HPTT/PMT enhances the polarization of the cathode as shown in Fig. 4(a and b). Specifically, the polarization potential is 0.59 V corresponding to a current density value of 0.1 A dm^{-2} in the VMS containing only 60 ppm Cl^-, 200 ppm PEP. The polarization potential is negatively shifted to 0.73 V as illustrated in Fig. 4(a) with addition of 6 ppm HPTT to the above electrolyte, compared with the polarization potential value of 0.68 V for PMT in Fig. 4(b). These results suggest that the inhibitory effect of PEP–HPTT is stronger than that of PEP–PMT. In addition, the convection-dependent polarization potential difference is not observed in Fig. 4(a and b), consistent with the results of GMs. The convection-dependent polarization potential difference is only observed when the composite inhibitor is present simultaneously with the accelerator.

Fig. 5 shows the Nyquist plot recorded at −0.65 V (*vs.* SMSE). The curves illustrated in Fig. 5 both contain two parts, a capacitive loop for the high frequency (HF) range and a capacitive loop for the low frequency (LF) range. According to previous reports,[31–33] the first capacitive loop (HF) indicates the $Cu^{2+} \rightarrow Cu^+$ reaction and the second capacitive loop (LF) is associated with the PEP–Cu^+–Cl^- relaxation and $Cu^+ \rightarrow Cu^0$ reaction. As shown in Fig. 5(b), the radius of both capacitive loops increases after the addition of 2 ppm HPTT, illustrating that the reduction of Cu^{2+} is more resistant and the PEP–Cu^+–Cl^- adsorption layer becomes more compact. This phenomenon becomes more obvious as the concentration of HPTT rises. In contrast, the radius of the two capacitance rings increases with the addition of PMT as seen in Fig. 5(a), but this increase is not as large as that of HPTT. These results imply that HPTT/PMT changes the nature of the PEP–Cu^+–Cl^- adsorption layer. Specifically, HPTT/PMT interacts with PEP, thereby enhancing the inhibition of copper deposition by PEP, consistent with the results of GMs and LSV measurements.

The equivalent circuit fitted the impedance data properly is displayed in Fig. 5. The electrochemical parameters obtained from the equivalent circuit are listed in Table 1. In this circuit, R_s is the solution resistance, C_{dl} is the double layer capacitance, R_1 is the charge transfer resistance corresponding to the $Cu^{2+} \rightarrow Cu^+$ reaction, C_f is the capacitance of adsorbed layer, and R_2 is the adsorbed layer resistance relevant to the $Cu^+ \rightarrow Cu^0$ reaction.[34,35] The addition of PMT/HPTT has little no effect on R_s. The values of R_1 and R_2 both increase with the gradual injection of PMT/HPTT, demonstrating that both levelers have the ability to inhibit the reduction of Cu^{2+}/Cu^+. It is worth noting that the R_1 and R_2 values increase by 260% and 1389% respectively after addition of 6 ppm HPTT, while the above factors of 6 ppm PMT are only 52% and 141%, respectively. These results suggest that the impact of HPTT on Cu^{2+}/Cu^+ reduction is far beyond PMT.

More importantly, the difference between the two levelers is only one phenolic hydroxyl group, so that the phenolic hydroxyl group becomes the key to improve the filling performance of this type of levelers.

3.2. Electroplating experiments

In order to investigate the filling performance of HPTT, electroplating experiments were conducted. The radius and depth

Table 2 Some molecular properties of HPTT and HPTT-iso calculated using DFT

	E_{HOMO} (eV)	E_{LUMO} (eV)	ΔE (eV)
HPTT	−5.966	−1.127	4.839
PMT	−6.105	−1.243	4.862

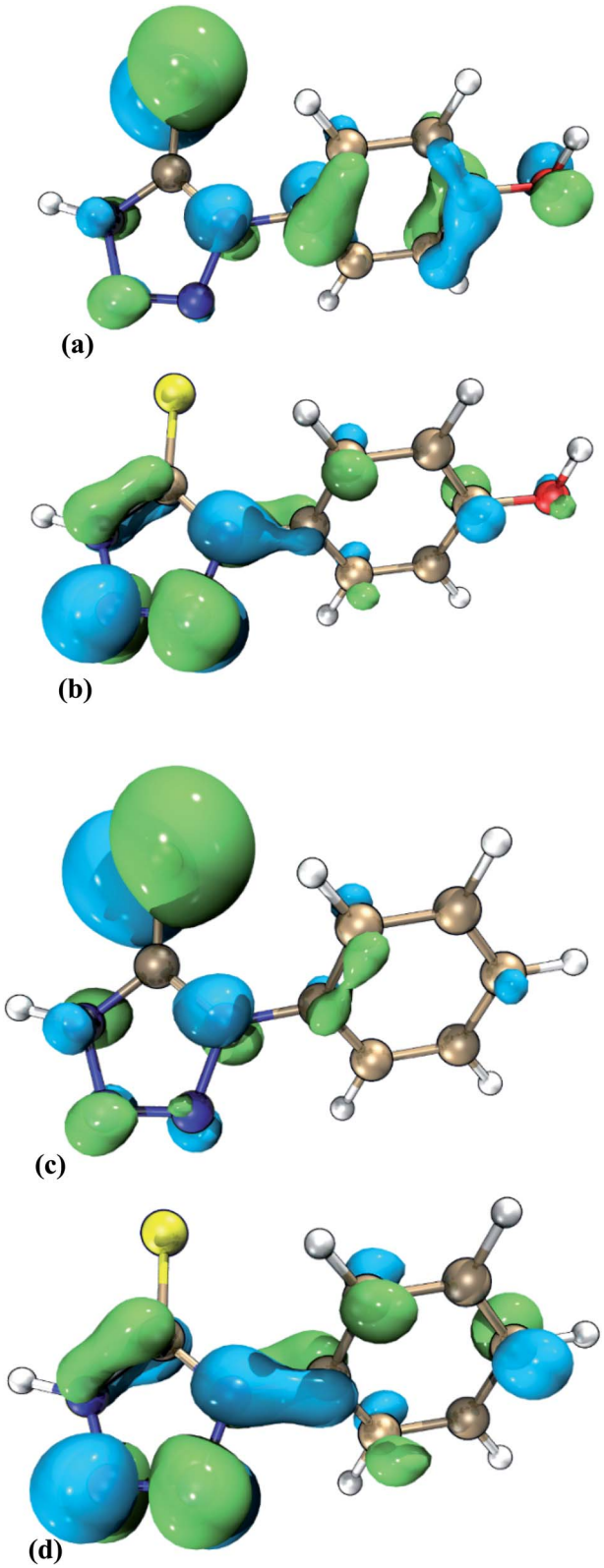

Fig. 7 The frontier molecular orbitals: HOMO of (a) HPTT, (c) PMT; LUMO of (b) HPTT, (d) PMT (dark blue: N, gold: C, red: O, yellow: S, white: H).

of microvias shown in Fig. 6 are 150 μm and 75 μm, respectively. Fig. 6(a and c) shows the cross-sections of microvias obtained by plating with PMT (a) and HPTT (c) as the leveler for 60 min, respectively. Plating solution with PMT as the leveler obtained the microvia with a filling rate (F) of 72.7% and the surface copper thickness equal to 25.57 μm, as displayed in Fig. 6(a). In contrast, the microvia shown in Fig. 6(c) filled with HPTT as the leveler achieved superfilling with a filling rate and the surface copper thickness of 95.6% and 17.97 μm, respectively. These results are consistent with the conclusion of the electrochemical test that the phenolic hydroxyl group in HPTT plays a key role in the filling process. The value of $\Delta\eta$ (HPTT) in GMs is larger than that of $\Delta\eta$ (PMT), indicating that the difference between the copper deposition rate inside and outside the microvia is larger when HPTT is used as the leveler, which is more favorable for superfilling.

Further electroplating experiments were carried out for HPTT with better filling performance. The plating durations for the microvia cross-sections shown in Fig. 6(b and d) are 40 min and 80 min, respectively, where the leveler is HPTT. The filling rate and surface copper thickness corresponding to the two time durations are 15.42 μm, 77.6% and 29.14 μm, 99.5%, respectively. In terms of the filling rate, the formulation is sufficient to fill the microvias with a radius of 150 μm and a depth of 75 μm in 60 min. No overfilling due to a large accumulation of SPS at the bottom of the microvia is observed, suggesting that the PEP–HPTT composite inhibitor can gradually replace the SPS adsorbed at the bottom with the enhancement of forced convection, thus preventing the occurrence of overfilling. In addition, a void-free filling is acquired in only 40 minutes for microvias with a diameter of 100 μm. The filling rate is 94.3% and the thickness on the surface is 14.10 μm.

3.3. Quantum chemical calculations and molecular dynamics simulation

The effect of the difference in functional groups between HPTT and PMT on the filling performance was further investigated by quantum chemical calculations. On the basis of the frontier orbital theory, HOMO and LUMO have the greatest impact on the adsorption of organic molecules on metals.[36] A small value of E_{LUMO} means a strong electron absorption capacity, while a large value of E_{HOMO} means a strong electron supply capacity. The E_{HOMO} values of HPTT and PMT are −5.966 eV and −6.105 eV respectively as marked in Table 2, indicating that HPTT is more capable of donating electrons to bind with the d-orbital of the metal.

HOMOs of HPTT and PMT are mainly distributed on sulfur atoms, as displayed in Fig. 7(a and c), indicating that sulfur atoms are the main electrophilic attack region. According to the previous report,[21] when the benzene ring is attached to an electron-donating group, the HOMO and LUMO energy levels increase simultaneously, but the HOMO energy level increases more. The electron donating ability of the hydroxyl group on benzene ring is stronger than that of the hydrogen atom on benzene ring, so that the E_{HOMO} and E_{LUMO} values of HPTT are higher than those of PMT. Moreover, smaller energy gap $\Delta E = E_{LUMO} - E_{HOMO}$ partially reflects the reactivity of the molecule.[37,38] As a result, ΔE (HPTT) < ΔE (PMT) also implies that the desorption of HPTT is more difficult, leading to the

predominance of PEP-HPTT in the competitive adsorption with SPS on the copper surface and more favorable inhibition of copper deposition outside microvias.

ESP plot is a straightforward visualization of the preferred reaction sites and powerful tool for predicting molecular properties. The low electron density (red) region represents the high ESP value and the high electron density (blue) region represents the low ESP value. Fig. 8(a and b) show that the high electron density region of HPTT and PMT is mainly distributed on N and S atoms, and the low electron density region is distributed on H atoms. Atoms in the high electron density region are generally considered to have a greater affinity for metal surfaces.[39,40] The electron density around the hydrogen atoms in HPTT is lower than that of PMT, and the maximum values of ESP (HPTT) and ESP (PMT) are about 50 kcal mol^{-1} and 40 kcal mol^{-1}, respectively, illustrating that HPTT is more easily attracted to the oxygen atom with high electron density on the inhibitor.

Steiner and Saenger considered a hydrogen bond as "any cohesive interaction X–H···Y where H carries a positive and Y a negative (partial or full) charge and the charge on X is more negative than on H".[41] According to the above definition of hydrogen bond, the H atoms of HPTT and PMT located in the low electron density region, as shown in Fig. 8, can form a hydrogen bond with the O atom of the inhibitor, densifying the adsorption layer. To further verify the binding state of HPTT/PMT with PEP, the quantum chemical calculations were performed to optimize several geometric configurations of the composite inhibitors, as marked in Fig. 9. The E_{ads} obtained from eqn (3) is referred to as the binding energy between a leveler molecule and a PEP molecule.

$$E_{ads} = E_{complex} - (E_{PEP} + E_{Leveler}) \quad (3)$$

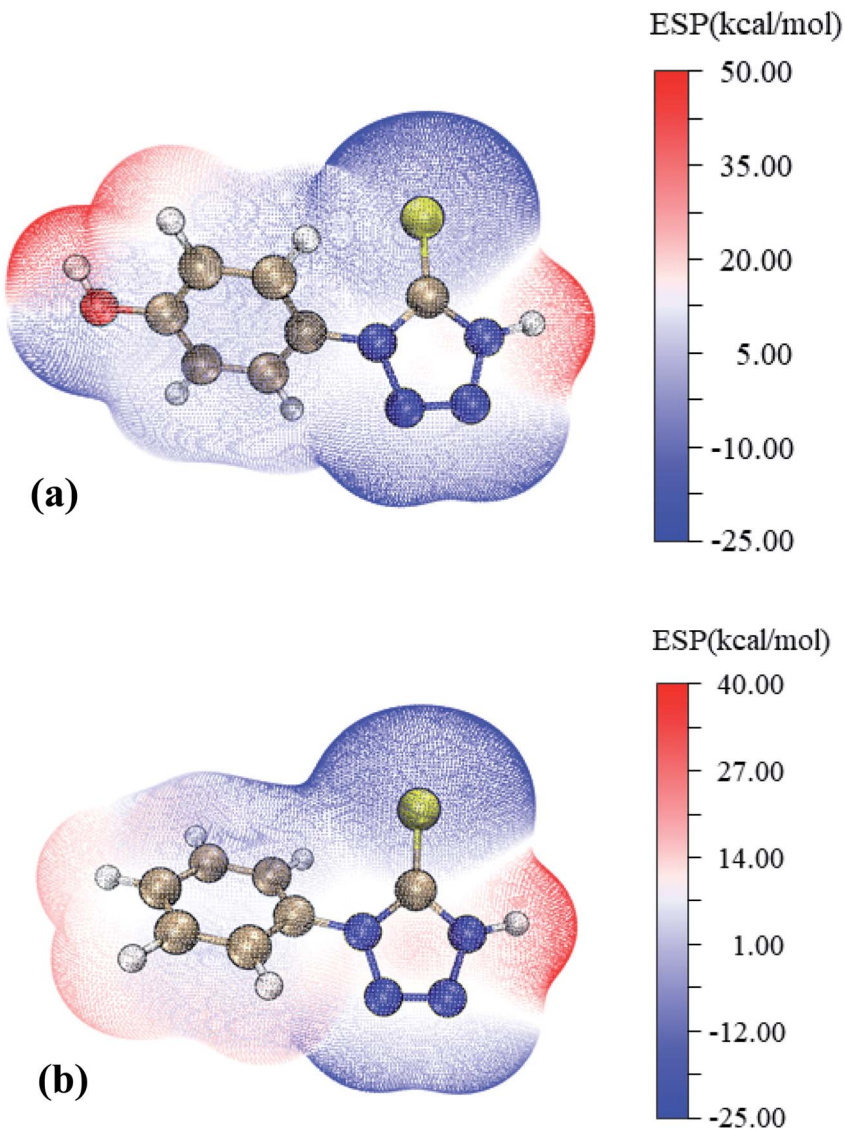

Fig. 8 ESP mapped molecular vdW surface of (a) HPTT, (b) PMT (dark blue: N, gold: C, red: O, yellow: S, white: H).

where $E_{complex}$ represents the total energy of the entire conformation, E_{PEP} represents the energy of a PEP molecule, and E_{HPTT} represents the energy of a leveler molecule. The binding energies of four structures are summarized in Table 3.

HPTT is mainly bonded to the O atom of PEP through the phenol hydroxyl (O–H···O) and nitrogen atoms (N–H···O) as illustrated in Fig. 9 (**9a**, **9b**). The E_{ads} of **9b** is lower than that of **9a**, attributed to the fact that the electronegativity of N atom is smaller than that of O atom. On the other hand, PMT can bind to the O atom of PEP through the H atom on the tetrazole ring and benzene ring, as shown in Fig. 9 (**9c**, **9d**). More importantly, both ends of these leveler molecules can be combined with PEP, allowing the leveler molecules to form a chain structure with PEP and facilitating multilayer adsorption of PEP on copper surfaces. Quantum chemical calculations show that the chain structure becomes stronger due to the introduction of phenolic hydroxyl group. The E_{ads} of both geometric configurations of PEP–HPTT are correspondingly larger than those of PEP–PMT, demonstrating that the adsorption capacity of PEP–HPTT on the copper surface would be stronger than that of PEP–PMT.

The model of PEP–SPS–HPTT electroplating system can be proposed based on the interactions of the additives, as illustrated in Fig. 10. Assuming that the diffusion of copper ions and the accelerator (SPS) is not restricted in the microvia, so that the concentrations of copper ion and SPS remain constant everywhere. For the inhibitor, the diffusion of PEP is limited by the large molecular volume, resulting in a lower concentration at the bottom of the microvia than on the surface. On the other hand, the PEP molecules adsorbed at the bottom are gradually replaced by SPS during the electrodeposition process, further reducing the concentration of PEP at the bottom. PEP–HPTT/PMT prevails in competitive adsorption with SPS outside the microvia due to the strong convection, thus strongly inhibiting copper deposition on the surface. At the same time, the bottom of the microvia is mainly occupied by SPS, where superfilling is allowed. In the absence of the leveler, the accumulation effect of SPS molecules would occur as the surface area inside the microvia gradually decreased.[9,42]

Nevertheless, this phenomenon is eliminated by the presence of a composite inhibitor (PEP–HPTT/PMT). The composite inhibitor gradually dominates in the competitive adsorption with SPS and replaces the SPS molecules inside the microvia as the filling process comes to an end, due to the gradual

Table 3 The binding energy of composite inhibitors calculated using Gaussian 09W

Structure	E_{ads} (kcal mol^{-1})
9a	−26.47
9b	−20.35
9c	−15.40
9d	−23.04

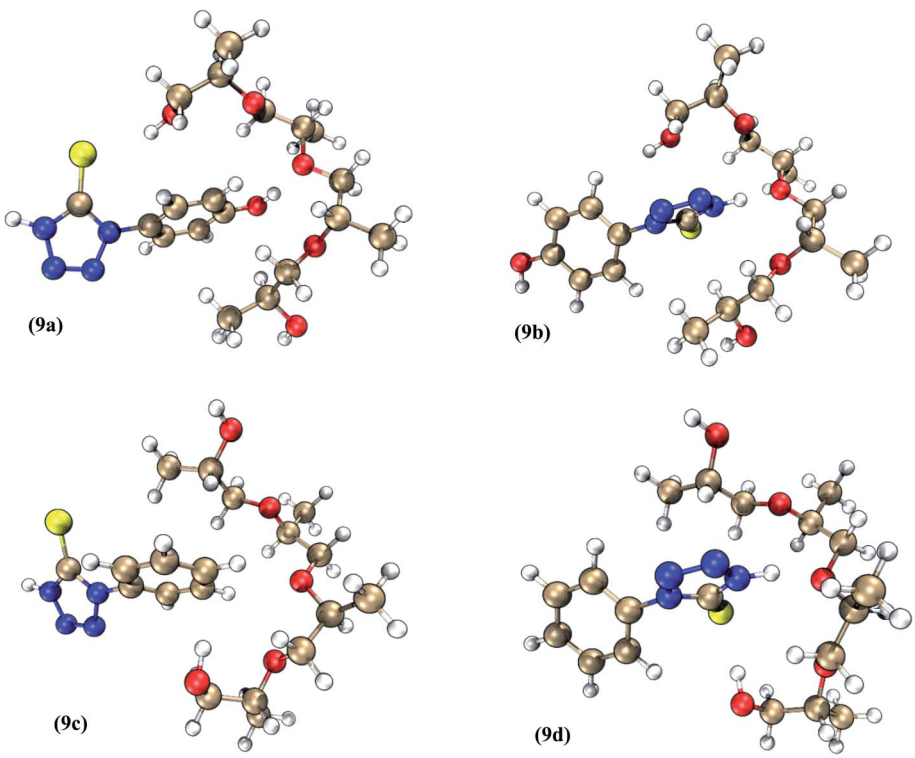

Fig. 9 Composite inhibitor models of (**9a**, **9b**) PEP–HPTT fragments and (**9c**, **9d**) PEP–PMT fragments (dark blue: N, gold: C, red: O, yellow: S, white: H).

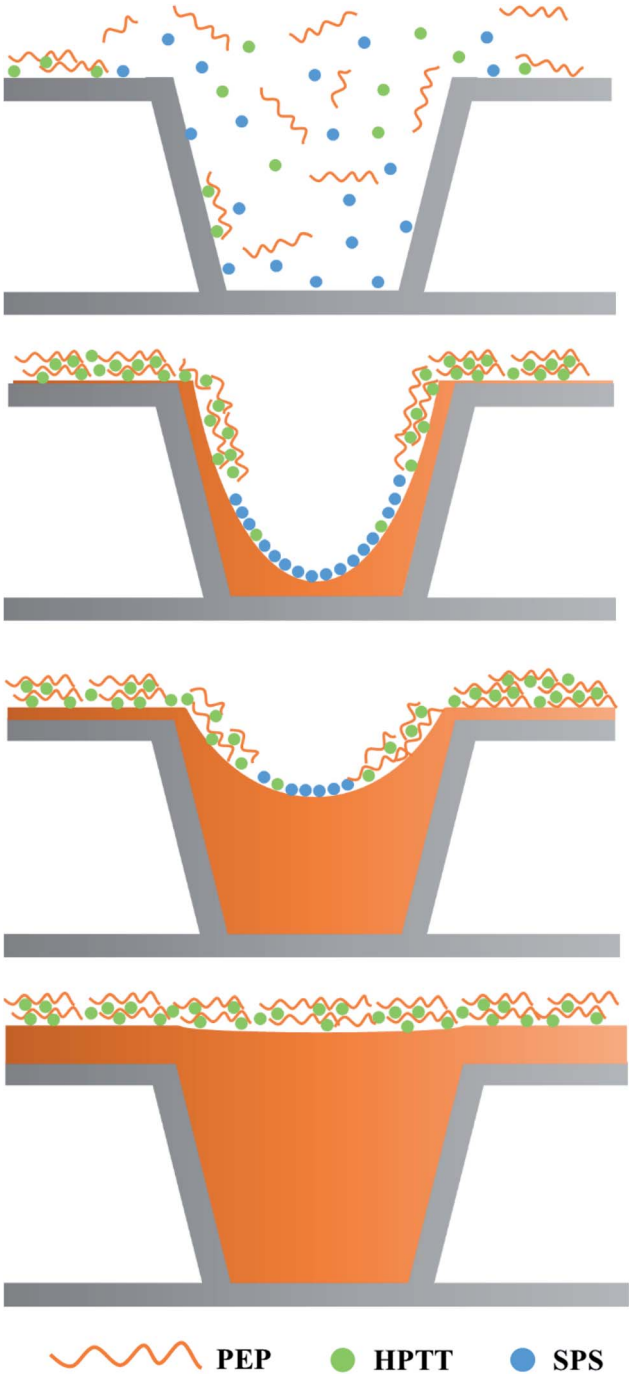

Fig. 10 The model of PEP–SPS–HPTT electroplating system.

enhancement of forced convection inside the microvia, eventually preventing the overfilling from happening.

4. Conclusion

It is found that a new tetrazole derivative HPTT is capable of filling microvias with a diameter of 150 μm and a depth of 75 μm in one hour in the PCB fabrication system. The plating experiments demonstrate that the complete filling of microvias can be achieved with the plating solution consisting of 0.88 mol L^{-1} $CuSO_4 \cdot 5H_2O$, 0.54 mol L^{-1} H_2SO_4, 60 ppm Cl^-, 200 ppm PEP, 4 ppm SPS and 6 ppm HPTT. The filling rate, surface copper thickness and plating time of the microvia with a diameter of 150 μm are 95.6%, 17.97 μm and 60 min respectively, while those of the microvia with a 100 μm diameter are 94.3% 14.10 μm and 40 min, respectively.

Electrochemical measurements suggest that a convection-dependent interaction between HPTT and PEP exists in the absence of Cl^-, and HPTT enhances the inhibition of copper deposition by PEP in the presence of Cl^-.

Quantum chemical calculations show that the active sites of HPTT are O, S, N atoms. HPTT can bond to with copper surface by sulfur atoms while bind to PEP *via* the phenolic hydroxyl group and hydrogen atom of tetrazole. The E_{ads} of PEP–HPTT in the same conformation is correspondingly larger than that of PEP–PMT, demonstrating that the adsorption capacity of PEP–HPTT on the copper surface would be stronger than that of PEP–PMT.

Conflicts of interest

There are no conflicts to declare.

Acknowledgements

The authors gratefully acknowledge the support of the National Natural Science Foundation of China (No. 61841401) and the Natural Science Foundation of Jiangxi Province of China (No. 20212BAB204046).

References

1 C.-F. Hsu, W.-P. Dow, H.-C. Chang and W.-Y. Chiu, Optimization of the Copper Plating Process Using the Taguchi Experimental Design Method I. Microvia Filling by Copper Plating Using Dual Levelers, *J. Electrochem. Soc.*, 2015, **162**, D525–D530.
2 S. Ren, Z. Lei and Z. Wang, Investigation of suppressor polyethylene glycol dodecyl ether on electroplated Cu filling by electrochemical method, *Trans. Inst. Met. Finish.*, 2015, **93**, 190–195.
3 Z. Lei, L. Chen, W. Wang, Z. Wang and C. Zhao, Tetrazole Derived Levelers for Filling Electroplated Cu Microvias: Electrochemical Behaviors and Quantum Calculations, *Electrochim. Acta*, 2015, **178**, 546–554.
4 Z. Lai, S. Wang, C. Wang, Y. Hong, Y. Chen, H. Zhang, G. Zhou, W. He, K. Ai and Y. Peng, Computational analysis and experimental evidence of two typical levelers for acid copper electroplating, *Electrochim. Acta*, 2018, **273**, 318–326.
5 S. Ren, Z. Lei and Z. Wang, Investigation of Nitrogen Heterocyclic Compounds as Levelers for Electroplating Cu Filling by Electrochemical Method and Quantum Chemical Calculation, *J. Electrochem. Soc.*, 2015, **162**, D509–D514.
6 J. G. Long, P. C. Searson and P. M. Vereecken, Electrochemical characterization of adsorption-desorption of the cuprous-suppressor-chloride complex during

electrodeposition of copper, *J. Electrochem. Soc.*, 2006, **153**, C258–C264.

7 A.-y. Wang, B. Chen, L. Fang, J.-j. Yu and L.-m. Wang, Influence of branched quaternary ammonium surfactant molecules as levelers for copper electroplating from acidic sulfate bath, *Electrochim. Acta*, 2013, **108**, 698–706.

8 T. M. T. Huynh, F. Weiss, N. T. M. Hai, W. Reckien, T. Bredow, A. Fluegel, M. Arnold, D. Mayer, H. Keller and P. Broekmann, On the role of halides and thiols in additive-assisted copper electroplating, *Electrochim. Acta*, 2013, **89**, 537–548.

9 W.-P. Dow, Y.-D. Chiu and M.-Y. Yen, Microvia Filling by Cu Electroplating Over a Au Seed Layer Modified by a Disulfide, *J. Electrochem. Soc.*, 2009, **156**, D155–D167.

10 W.-P. Dow, C.-C. Li, Y.-C. Su, S.-P. Shen, C.-C. Huang, C. Lee, B. Hsu and S. Hsu, Microvia filling by copper electroplating using diazine black as a leveler, *Electrochim. Acta*, 2009, **54**, 5894–5901.

11 R. Manu and S. Jayakrishnan, Effect of organic dye on copper metallization of high aspect ratio through hole for interconnect application, *Mater. Chem. Phys.*, 2012, **135**, 425–432.

12 B. Bozzini, C. Mele, L. D'Urzo and V. Romanello, An electrochemical and in situ SERS study of Cu electrodeposition from acidic sulphate solutions in the presence of 3-diethylamino-7-(4-dimethylaminophenylazo)-5-phenylphenazinium chloride (Janus Green B), *J. Appl. Electrochem.*, 2006, **36**, 973–981.

13 C. Chang, X. Lu, Z. Lei, Z. Wang and C. Zhao, 2-Mercaptopyridine as a new leveler for bottom-up filling of micro-vias in copper electroplating, *Electrochim. Acta*, 2016, **208**, 33–38.

14 H.-C. Tsai, Y.-C. Chang and P.-W. Wu, Rapid Galvanostatic Determination on Levelers for Superfilling in Cu Electroplating, *Electrochem. Solid-State Lett.*, 2010, **13**, D7–D10.

15 Y. Qiang, S. Zhang, S. Xu and W. Li, Experimental and theoretical studies on the corrosion inhibition of copper by two indazole derivatives in 3.0% NaCl solution, *J. Colloid Interface Sci.*, 2016, **472**, 52–59.

16 S.-M. Huang, C.-W. Liu and W.-P. Dow, Effect of Convection-Dependent Adsorption of Additives on Microvia Filling in an Acidic Copper Plating Solution, *J. Electrochem. Soc.*, 2012, **159**, D135–D141.

17 W. P. Dow and C. W. Liu, Evaluating the filling performance of a copper plating formula using a simple galvanostat method, *J. Electrochem. Soc.*, 2006, **153**, C190–C194.

18 I. Tabakovic, S. Riemer and M. Sun, Self-Assembled Monolayer of 3-N, N-Dimethylaminodithiocarbamoyl-1-Propanesulfonic Acid (DPS) Used in Electrodeposition of Copper, *J. Electrochem. Soc.*, 2013, **160**, D3197–D3205.

19 M. Tang, S. Zhang, Y. Qiang, S. Chen, L. Luo, J. Gao, L. Feng and Z. Qin, 4,6-Dimethyl-2-mercaptopyrimidine as a potential leveler for microvia filling with electroplating copper, *RSC Adv.*, 2017, **7**, 40342–40353.

20 C. Liao, S. Zhang, S. Chen, Y. Qiang, G. Liu, M. Tang, B. Tan, D. Fu and Y. Xu, The effect of tricyclazole as a novel leveler for filling electroplated copper microvias, *J. Electroanal. Chem.*, 2018, **827**, 151–159.

21 J. Li, J. Xu, X. Wang, X. Wei, J. Lv and L. Wang, Novel 2,5-bis(6-(trimethylamonium)hexyl)-3,6-diaryl-1,4-diketopyrrolo 3,4-c pyrrole pigments as levelers for efficient electroplating applications, *Dyes Pigm.*, 2021, **186**, 109064.

22 W. P. Dow, M. Y. Yen, W. B. Lin and S. W. Ho, Influence of molecular weight of polyethylene glycol on microvia filling by copper electroplating, *J. Electrochem. Soc.*, 2005, **152**, C769–C775.

23 C. Lee, W. Yang and R. G. Parr, Development of the Colle-Salvetti correlation-energy formula into a functional of the electron density, *Phys. Rev. B: Condens. Matter Mater. Phys.*, 1988, **37**, 785–789.

24 T. Lu and F. Chen, Multiwfn: a multifunctional wavefunction analyzer, *J. Comput. Chem.*, 2012, **33**, 580–592.

25 Y.-D. Chiu and W.-P. Dow, Accelerator Screening by Cyclic Voltammetry for Microvia Filling by Copper Electroplating, *J. Electrochem. Soc.*, 2013, **160**, D3021–D3027.

26 P. Broekmann, A. Fluegel, C. Emnet, M. Arnold, C. Roeger-Goepfert, A. Wagner, N. T. M. Hai and D. Mayer, Classification of suppressor additives based on synergistic and antagonistic ensemble effects, *Electrochim. Acta*, 2011, **56**, 4724–4734.

27 H. Tu, P. Yen, S. Chen, S. Yau, W.-P. Dow and Y.-L. Lee, In Situ STM Imaging of Bis-3-sodiumsulfopropyl-disulfide Molecules Adsorbed on Copper Film Electrodeposited on Pt(111) Single Crystal Electrode, *Langmuir*, 2011, **27**, 6801–6807.

28 N. T. M. Hai, T. T. M. Huynh, A. Fluegel, M. Arnold, D. Mayer, W. Reckien, T. Bredow and P. Broekmann, Competitive anion/anion interactions on copper surfaces relevant for Damascene electroplating, *Electrochim. Acta*, 2012, **70**, 286–295.

29 W. P. Dow, H. S. Huang, M. Y. Yen and H. H. Chen, Roles of chloride ion in microvia filling by copper electrodeposition - II. Studies using EPR and galvanostatic measurements, *J. Electrochem. Soc.*, 2005, **152**, C77–C88.

30 Z. Tao, W. He, S. Wang, X. He, C. Jiao and D. Xiao, Synergistic Effect of Different Additives on Microvia Filling in an Acidic Copper Plating Solution, *J. Electrochem. Soc.*, 2016, **163**, D379–D384.

31 C. Gabrielli, P. Mocoteguy, H. Perrot, D. Nieto-Sanz and A. Zdunek, A model for copper deposition in the damascene process, *Electrochim. Acta*, 2006, **51**, 1462–1472.

32 Y.-B. Li, W. Wang and Y.-L. Li, Investigations on the invalidated process and related mechanism of PEG during copper via-filling process, *Appl. Surf. Sci.*, 2009, **255**, 3977–3982.

33 H. Cao, T. Hang, H. Ling and M. Li, Behaviors of Chloride Ions in Methanesulfonic Acid Bath for Copper Electrodeposition of Through-Silicon-Via, *J. Electrochem. Soc.*, 2013, **160**, D146–D149.

34 M. E. H. Garrido and M. D. Pritzker, EIS and statistical analysis of copper electrodeposition accounting for multi-component transport and reactions, *J. Electroanal. Chem.*, 2006, **594**, 118–132.

35 C. P. Fabian, M. J. Ridd, M. E. Sheehan and P. Mandin, Modeling the Charge-Transfer Resistance to Determine the Role of Guar and Activated Polyacrylamide in Copper Electrodeposition, *J. Electrochem. Soc.*, 2009, **156**, D400–D407.

36 C. Wang, A. J. Turinske and Y. Gao, Orientation-dependent ionization potential of CuPc and energy level alignment at C-60/CuPc interface, *Appl. Phys. B: Lasers Opt.*, 2013, **113**, 361–365.

37 C. Wang, J. Zhang, P. Yang and M. An, Electrochemical behaviors of Janus Green B in through-hole copper electroplating: an insight by experiment and density functional theory calculation using Safranine T as a comparison, *Electrochim. Acta*, 2013, **92**, 356–364.

38 G. Gece, The use of quantum chemical methods in corrosion inhibitor studies, *Corros. Sci.*, 2008, **50**, 2981–2992.

39 X. R. Ni, Y. M. Chen, X. F. Jin, C. Wang, Y. Z. Huang, Y. Hong, X. H. Su, G. Y. Zhou, S. X. Wang, W. He and Q. G. Chen, Investigation of polyvinylpyrrolidone as an inhibitor for trench super-filling of cobalt electrodeposition, *J. Taiwan Inst. Chem. Eng.*, 2020, **112**, 232–239.

40 R. Fu, T. Lu and F.-W. Chen, Comparing Methods for Predicting the Reactive Site of Electrophilic Substitution, *Acta Phys.-Chim. Sin.*, 2014, **30**, 628–639.

41 T. Steiner and W. Saenger, Role of C-H···O hydrogen-bonds in the coordination of water-molecules - analysis of neutron-diffraction data, *J. Am. Chem. Soc.*, 1993, **115**, 4540–4547.

42 H. P. Zhu, Q. S. Zhu, X. Zhang, C. Z. Liu and J. J. Wang, Microvia Filling by Copper Electroplating Using a Modified Safranine T as a Leveler, *J. Electrochem. Soc.*, 2017, **164**, D645–D651.